

# Supporting Information

Jönsson et al. 10.1073/pnas.1202858109

## SI Text

**Experimental Procedure. Preparation of the glass surfaces.** A glass slide (size no. 1: 0.13 mm in thickness, VWR International, Lut-terworth, UK) was cleaned in a (3:1 by volume) mixture of con- centrated sulfuric acid (>95%; Fisher Scientific, Loughborough, UK) and 30% hydrogen peroxide (100 vols; Breckland Scientific Supplies, Thetford, UK) for 5 min (4 min of swirling followed by 1 min in an ultrasound bath). The sample was then thoroughly rinsed with Milli-Q™ water (Millipore, Billerica, MA) and dried with nitrogen gas. The cleaned glass slide was glued to the bottom of a Petri dish (diam. 35 mm, height 10 mm; Nunc, Roskilde, Denmark) using acetoxy silicone glue (Dow Corning 781; Dow Corning, Seneffe, Belgium). A hole with a diameter of 3 mm had been drilled in the bottom of the dish, which together with the glass slide make up a second, smaller, well in the Petri dish. The formation of the supported lipid bilayer (SLB) on the glass was typically made within 5 min after the glass slide had been glued to the Petri dish.

**Vesicle preparation.** Lipid vesicles were prepared by extrusion through a 50-nm membrane (Whatman, Maidstone, UK) using an Avanti Mini-Extruder (Avanti Polar Lipids, Alabaster, AL). The vesicles consisted of 1-palmitoyl-2-oleoyl-*sn*-glycero-3-phos- phocholine (POPC) from Avanti Polar Lipids with either 0 or 0.1 wt% of 1,2-dipalmitoyl-*sn*-glycero-3-phosphoethanolamine- N-(cap biotinyl) (biotin-PE; Avanti Polar Lipids). Lipid vesicles made of POPC and 1 wt% of Oregon Green® 488 1,2-dihexade- canoyl-*sn*-glycero-3-phosphoethanolamine (OG-DHPE; Invitro- gen, Carlsbad, CA) were also prepared using the same procedure. The buffer solution used in all experiments was a mixture of 125 mM NaCl (Breckland Scientific Supplies), 10 mM tris [hydroxymethyl]aminomethane (TRIS; Pharmacia Biotech, Up- psala, Sweden) and 1 mM ethylenediaminetetraacetic acid di- sodium salt dihydrate (EDTA; Pharmacia Biotech), with a pH of 7.4. To reduce clogging in the pipette by larger particles the buffer solution was filtered through a 0.2 μm membrane (AnaChem, Luton, UK) before use. The fusion of the biotin-containing lipid vesicles into a fluid SLB was observed to be more reproducible when using this type of buffer than when using a buffer with 100 mM NaCl, 10 mM TRIS and 1 mM EDTA at a pH of 8.0, which often is used in SLB formation from vesicles (1, 2). In addition, when using 1×PBS buffer (phosphate buffered saline buffer at a pH of 7.4) fluid SLBs were reproducibly formed, but these SLBs had many nonruptured vesicles on the surface. Thus, the chosen buffer solution was a good comprise resulting in fluid SLBs with a reduced number of nonruptured vesicles on the surface/SLB.

**Formation of a lipid bilayer.** An SLB was formed by placing a 20 μl drop of the vesicle solution on the glass surface. For the protein experiments the vesicle solutions used consisted either of pure 0.1 wt% biotin-PE vesicles or a (1:1), (1:4), or (1:9) by volume mixture of 0.1 wt% biotin-PE vesicles and POPC vesicles. Assuming that the vesicles containing biotin-PE and the pure POPC vesicles will rupture into an SLB in approximately the same rate this will result in an SLB with approximately 0.05 wt%, 0.02 wt% and 0.01 wt% biotin-PE for the different mixtures, respectively. After 30 min, the vesicle suspension was replaced with a buffer solution by first withdrawing most of the liquid from the Petri dish and then adding 500 μl of the buffer solution. This was repeated three times to ensure that most of the lipid vesicles had been rinsed away.

After formation of the biotin-PE SLB, the buffer solution was exchanged with a 10 μg/ml (approximately 170 nM) protein so- lution. The protein streptavidin (SA), labeled with the fluorescent group Oregon Green® 488, was acquired from Invitrogen and bind to biotin-PE in the SLB. The binding of fluorescently labeled SA to the SLB was monitored in real time by total internal reflec- tion fluorescence (TIRF) microscopy. After 30 min the binding of SA to the SLB had reached equilibrium and the protein solu- tion was replaced by buffer solution. The fluorescence intensity from SA in the SLB did not change significantly during an experi- ment, indicating that the surface coverage of SA was approxi- mately the same.

**The microscopy setup.** The fluorescently labeled molecules were studied with an inverted Nikon Eclipse TE200 microscope (Ni- kon Corporation, Tokyo, Japan), using a Photometrics Cascade II:512 EMCCD camera (Photometrics, Tucson, AZ), and a 60× magnification (Plan Apo TIRF, NA = 1.45) oil immersion objective (Nikon Corporation). The acquired images consisted of 512 × 512 pixels with a pixel size of 0.11 × 0.11 μm in the sam- ple plane. For the illumination a 20 mW Cyan diode laser oper- ating at a wavelength of 488 nm (model no. PC13589; Spectra Physics, Ontario, Canada) was used and focused on the sample plane of the microscope in epifluorescence mode. By moving the point at which the laser enters the objective, it was possible to switch between epi-mode (the laser beam being aligned to the center of the objective) and TIRF-mode (the laser beam being aligned towards the side of the objective). The images were acquired using time-lapse acquisition, with an exposure time of 100 ms, and a time between frames of either 2 s or 15 s, where the faster frame rate was used to monitor the kinetic behavior of the trap. All measurements were made at ambient temperature, about 22 °C.

**Positioning the pipette above the surface.** Conical glass pipettes were pulled from borosilicate glass capillaries with an inner di- ameter of 0.5 mm and an outer diameter of 1.0 mm (BF100-50-10; Intracel, Royston, UK). The pulling was made with a laser-based pipette puller (Model P-2000; Sutter Instruments, Novato, CA) with the default program #11, typically resulting in pipettes with a tip radius between 1–1.5 μm and a half-cone angle of 3–4°. The pipettes were filled approximately half way with buffer solution using a MicroFil™ syringe needle for filling micropipettes (World Precision Instruments, Sarasota, FL). The pipettes were mounted in a pipette and electrode holder from Harvard Apparatus (ESW- F10P; Harvard Apparatus, Kent, UK). This holder was in turn mounted on a custom-made holder on the inverted microscope, which could be moved in the *x*-, *y*-, and *z*-direction by a piezoelec- tric three-dimensional positioning system (Tritor 38; Piezosystem Jena, Jena, Germany). The pipette was illuminated from the side with a torch and the shadow of the pipette was observed in the microscope. The shadow was in turn used to position the pipette at the center of the field of view in the microscope and at a dis- tance of 5–10 μm above the surface. To bring the pipette to within one tip radius of the surface the ion current between an Ag/AgCl electrode in the pipette and an Ag/AgCl reference electrode in the bath outside of the pipette was measured. A voltage of 40 mV was applied to the electrode in the pipette and the current be- tween the two electrodes was amplified by a home-built amplifier with a gain of about 100 MΩ. The effect of electrophoretic and electroosmotic forces on the accumulation of molecules in the SLB could be neglected in the experiments. The amplified signal

was passed through a low-pass filter (Frequency devices 902; Frequency Devices, Ottawa, IL) after which the filtered signal was monitored by a PC-based digital oscilloscope (Picoscope ADC-212; Pico Technology, St Neots, UK). The pipette was brought closer to the surface with the piezoelectric positioning system until the current to the oscilloscope had dropped by typically 1–2%. Even though overall drifts of the ion current larger than 1–2% of the initial signal could take place during an experiment, the relative change in current when moving the pipette rapidly away from the surface was approximately the same.

**Applying pressure.** The pipette holder from Harvard Apparatus contains a side port to which silicon tubing could be connected. The tubing was in turn connected to a 10-ml syringe whose position was controlled via a stepper motor (C-862 Mercury; Physik Instrumente, Karlsruhe, Germany). By moving the stepper motor the pressure in the tubing, and thus at the top of the pipette, could be altered and controlled from a custom-written LabVIEW 2009 program (National Instruments, Newbury, UK). The pressure in the tubing was measured in real-time by a home-made pressure sensor that sent the pressure to the LabVIEW program. This, in turn, acted as feedback to maintain a fixed pressure in the system. For the accumulation experiments a hydrostatic pressure between –0.5 to –20 kPa was applied at the top of the pipette. When turning off the trap, the pipette was first rapidly moved away from the surface after which the applied pressure was turned off.

**Analysis of the Data. Characterization of the pipettes.** A snapshot of the tip of the pipette was acquired by optical microscopy using a 20× air objective, with the axis of the pipette being in the sample plane of the microscope (see Fig. S1). The dashed lines in Fig. S1 delineate the outer walls of the pipette. From Fig. S1 the outer cone angle,  $2\theta_1$ , was measured to 10.8°. By using the expression:

$$\tan(\theta) = \tan(\theta_1) R_{\text{inner}}/R_{\text{outer}}, \quad [\text{S1}]$$

this gives an inner half-cone angle of the pipette of  $\theta = 2.7^\circ$ , where the ratio between the inner and outer radius of the pipette is assumed to be  $R_{\text{inner}}/R_{\text{outer}} = 0.5$ , the same value as the ratio between the inner and outer radius of the capillary before the pipette was pulled. From Fig. S1 the inner radius of the pipette tip was measured to  $R_0 \approx 1.5 \mu\text{m}$ . The inner pipette radius can also be estimated from the ion current through the pipette, when immersed in an electrolyte, using Eq. S2 (3, 4):

$$R_{\text{pipette}} \approx \frac{1}{\pi K R_0 \tan(\theta)}. \quad [\text{S2}]$$

The electric resistance over the pipette,  $R_{\text{pipette}}$ , was here  $\sim 3.46 \text{ M}\Omega$ , which with an ion conductivity  $K = 1.6 \text{ S/m}$  for an electrolyte containing 125 mM NaCl (5), gives  $R_0 \approx 1.2 \mu\text{m}$ , similar to the value obtained from the micrograph in Fig. S1. One reason for the slightly different values may be that the half-cone angle of the pipette changes somewhat along the length of the pipette, which is not accounted for by Eq. S2.

**Analysis of the accumulation.** In the images acquired by the EMCCD camera there is always a signal which does not arise from fluorescent SA, but instead is due to dark counts in the camera and autofluorescence from the glass surface. To estimate this value a snap shot of the lipid bilayer was taken before the protein molecules were added. The value obtained was thereafter subtracted from all subsequent images. After fluorescently labeled SA had been added one or several images of the SLB was acquired when the pressure to the pipette was turned off and the pipette was far from the surface. This was used as background to account for a nonuniform illumination profile. All subsequent

images were divided by the background image. To compensate for bleaching during the experiments each image was normalized with the intensity at the edge of the image, which was sufficiently far away from the area of the trap not to be affected by the hydrodynamic forces. This results in the relative intensity of the images being one outside of the trap.

The center of mass position of the accumulated molecules was determined from an image taken after the trap had been turned on. A line profile along the  $x$ direction of the image, averaged over 4–8 pixels in the  $y$ direction around the center of mass position, was taken for all images. To determine the amplitude of the accumulation at  $r = 0$  a Gaussian curve was fitted to the line profile, and the amplitude of the fit was used to give the relative intensity beneath the tip of the pipette.

**The Surface Coverage of Proteins in the SLB.** To estimate the surface coverage,  $\Gamma$ , of protein molecules in the SLB it is assumed that all receptors in the upper monolayer of the SLB have bound a protein. The surface coverage of SA is then given by:

$$\Gamma = \chi_r/nA_{\text{lipid}}, \quad [\text{S3}]$$

where  $\chi_r$  is the molar fraction of receptors in the upper monolayer,  $n$  is the number of biotin-PE anchors per SA and  $A_{\text{lipid}}$  is the cross-sectional area of a lipid molecule. The molar fraction of biotin-PE in the upper monolayer of the SLB is  $\chi_r = 0.072 \text{ mol}\%$  for an SLB with 0.1 wt% biotin-PE. It is here assumed that biotin-PE distributes equally between both monolayers of the SLB and that the mass of a POPC molecule and a biotin-PE molecule is 760 Da and 1053 Da, respectively. Assuming that  $n = 1$  (6), and that  $A_{\text{lipid}} = 0.63 \text{ nm}^2$  (7), this results in a surface concentration of SA of  $\Gamma(0.1 \text{ wt}\%) = 1.15 \times 10^{-3} \text{ proteins/nm}^2$ . With a cross-sectional area of a SA molecule of  $25 \text{ nm}^2$  (8), this corresponds to a surface coverage of 2.84%.

From the intensity of the fluorescently labeled proteins the relative amount of SA for the different mixtures of biotin-PE vesicles and POPC vesicles could be estimated. Compared to the case with only 0.1 wt% biotin-PE vesicles the relative intensity for the (1:1) mixture was  $0.49 \pm 0.05$  ( $n = 6$ ), for the (1:4) mixture it was  $0.28 \pm 0.02$  ( $n = 4$ ) and for the (1:9) mixture it was  $0.10 \pm 0.01$  ( $n = 6$ ). The values are here given as the average value  $\pm$  one standard deviation obtained from  $n$  measurements. Thus, the amount of SA bound to the surface scales, more or less, linearly with the amount of biotin-PE vesicles in the biotin-PE: POPC mixtures.

**The Hydrodynamic Force Acting on a Single Protein.** To obtain an order of magnitude estimate of the hydrodynamic force on a single protein,  $F_{\text{hydro}}$ , we assume that at low surface coverage each protein can be approximated as an anchored sphere with a hydrodynamic force given by the Stokes-Einstein relation:

$$F_{\text{hydro}} \approx 6\pi\eta R_c v_b, \quad [\text{S4}]$$

where  $\eta$  is the viscosity of the liquid,  $R_c = (3V_{\text{SA}}/4\pi)^{1/3}$  is the effective radius of the protruding part of the protein and  $v_b$  is the effective velocity felt by the protein from the bulk flow. If  $v_b$  is approximated with the velocity of the bulk flow a distance  $h_c/2$  from the upper surface of the SLB, with  $h_c$  being the approximate height of the protruding part of the protein, this gives:

$$v_b \approx \frac{\sigma_{\text{hydro}}}{2\eta} h_c, \quad [\text{S5}]$$

where  $\sigma_{\text{hydro}}$  is the shear stress on the surface. The expression in Eq. S5 inserted into Eq. S4 gives:

$$F_{\text{hydro}} \approx 3\pi\sigma_{\text{hydro}} R_c h_c. \quad [\text{S6}]$$

For high surface coverage the protein molecules will shield the sides of each other from the hydrodynamic flow. Thus, only the upper surface of the proteins will experience a drag force, which is approximately given by:

$$F_{\text{hydro}} \approx \pi R_c^2 \sigma_{\text{hydro}}. \quad [\text{S7}]$$

Both Eq. S6 and Eq. S7 are proportional to  $\sigma_{\text{hydro}}$  and the size of a protein molecule squared, but with different proportionality constants. Thus, the hydrodynamic force can, as a first approximation, be written as:

$$F_{\text{hydro}} = \alpha 3\pi R_c h_c \sigma_{\text{hydro}}, \quad [\text{S8}]$$

where  $\alpha$  is roughly equal to 1 for low surface coverage and  $R_c/3h_c$  for high surface coverage.

**Simulations.** Numerical simulations were made using COMSOL Multiphysics® 4.2 (COMSOL AB, Stockholm, Sweden), a program that solves partial differential equations using the finite element method. The simulations were made for the geometry shown in Fig. S2, utilizing the cylindrical symmetry to transform the three-dimensional problem to a set of partial differential equations in two dimensions.

**Simulation of the ion current.** The electrical potential in the system is described by Laplace's equation:

$$0 = \nabla^2 \Psi. \quad [\text{S9}]$$

Eq. S9 was solved using the Electrostatics module in COMSOL Multiphysics. The following boundary conditions were used (see Fig. S2 for the numbering of boundaries): 1, axial symmetry; 2,  $\Psi = V_0$ ; 3,  $\Psi = 0$ ; and the other boundaries had the "zero charge" condition ( $\mathbf{n} \cdot \nabla \Psi = 0$ , where  $\mathbf{n}$  is a normal vector to the boundary). The ion current,  $I$ , through the pipette is given by:

$$I = \int (-K \nabla \Psi) \cdot \mathbf{n} dA, \quad [\text{S10}]$$

where the integral is over a cross-section of the pipette,  $K$  is the ion conductivity of the electrolyte solution and  $\mathbf{n}$  is a normal vector to the cross-sectional surface. The total voltage drop over the pipette,  $V_{\text{tot}}$ , is given by (see also Eq. S2):

$$V_{\text{tot}} = V_0 + I/(\pi K R_{\text{top}} \tan(\theta)), \quad [\text{S11}]$$

where  $R_{\text{top}}$  is the inner radius of the pipette at  $z = 50R_0 + h$  in Fig. S2 (the length of boundary 2). From this expression the total resistance over the pipette can be calculated as  $R_{\text{pipette}} = V_{\text{tot}}/I$ , which for a fixed value of  $V_{\text{tot}}$  will increase when  $h$  is decreased. As an example, for a pipette with  $\theta = 2.7^\circ$ ,  $R_0 = 1.5 \mu\text{m}$  and  $R_1 = 3.0 \mu\text{m}$  the value of  $R_{\text{pipette}}$  increases by 1.3% when the distance to the surface is changed from  $10R_0$  to  $R_0$ .

**Simulation of the hydrodynamic flow.** The flow velocity,  $\mathbf{u}$ , and the pressure,  $p$ , are given by Navier-Stokes equations for an incompressible flow:

$$0 = -\nabla p + \eta \nabla^2 \mathbf{u} \quad [\text{S12}]$$

and

$$\nabla \cdot \mathbf{u} = 0, \quad [\text{S13}]$$

where  $\eta$  is the viscosity of the liquid ( $\eta = 1 \text{ mPa s}$  was used in the simulations). Eq. S12 and Eq. S13 were solved using the Creeping flow module in COMSOL Multiphysics. The following boundary conditions were used (see Fig. S2 for the numbering of boundaries): 1, axial symmetry; 2, a velocity function given by:

$$\mathbf{u} = -\frac{2(R_{\text{top}}^2 - r^2)Q}{\pi R_{\text{top}}^4} \mathbf{e}_z, \quad [\text{S14}]$$

where  $Q$  is the flow rate through the pipette and  $\mathbf{e}_z$  is a unit vector in the  $z$ -direction and  $p = 0$  and no viscous stress. A no-slip condition was used at all other boundaries. The flow rate  $Q$  is related to the total pressure drop over the pipette,  $\Delta p$ , by (3):

$$\Delta p = p_{\text{top}} + \frac{8\eta Q}{3\pi R_{\text{top}}^3 \tan(\theta)}, \quad [\text{S15}]$$

where  $p_{\text{top}}$  is the average pressure at boundary 2 in Fig. S2. For a pipette with  $\theta = 2.7^\circ$ ,  $R_0 = 1.5 \mu\text{m}$ ,  $R_1 = 3.0 \mu\text{m}$  and  $h = R_0$  a total pressure drop of  $-1 \text{ kPa}$  give rise to a flow rate of  $Q = 150 \text{ pl/s}$ , which was used as input value to Eq. S14 for the boundary condition at boundary 2.

The hydrodynamic shear stress on the surface at  $z = 0$  is given by:

$$\sigma_{\text{hydro}} = \eta \left. \frac{\partial u_r}{\partial z} \right|_{z=0}, \quad [\text{S16}]$$

where  $u_r$  is the  $r$ -component of the flow velocity.

**Simulation of the concentration of molecules in the trap.** The following equations were used to simulate the time dependence on the concentration,  $c$ , of the protein molecules in the SLB under the action of the hydrodynamic forces (see also Eq. 4 and Eq. 7):

$$\frac{\partial c}{\partial t} = -\frac{1}{r} \frac{\partial}{\partial r} (r J_r), \quad [\text{S17}]$$

where

$$J_r = -D \frac{c_{\text{max}}}{c_{\text{max}} - c} \frac{\partial c}{\partial r} + \frac{D}{k_B T} c F_{\text{hydro}} \quad [\text{S18}]$$

and  $D$  is the diffusivity of the protein molecules in the lipid bilayer and  $c_{\text{max}}$  is an effective parameter to be fitted.  $F_{\text{hydro}}$  was given by the expression in Eq. S8, where  $\sigma_{\text{hydro}}$  at different radial positions on the surface was imported from the solution to the hydrodynamic flow simulation. The parameters  $R_c$  and  $h_c$  were chosen as 3.1 nm and 5 nm, respectively, based on crystallography data for SA from Darst, et al. (8). Eq. S17 was then solved using a one-dimensional time-dependent PDE module in COMSOL Multiphysics. The hydrodynamic force was scaled by the pressure that had been applied over the pipette at different times. The parameters  $c_{\text{max}}$  and  $\alpha$  were determined by fitting a line profile of the fluorescence intensity from SA at steady state (see the solid line in Fig. 3B) to the analytical expression in Eq. 8. The diffusivity of the proteins was then determined from fitting the decrease in intensity at  $r = 0$  as a function of time when the trap had been turned off.

- Jonsson P, Beech JP, Tegenfeldt JO, Hook F (2009) Shear-driven motion of supported lipid bilayers in microfluidic channels. *J Am Chem Soc* 131:5294–5297.
- Jonsson P, Jonsson MP, Tegenfeldt JO, Hook F (2008) A method improving the accuracy of fluorescence recovery after photobleaching analysis. *Biophys J* 95:5334–5348.

- Sanchez D, et al. (2008) Noncontact measurement of the local mechanical properties of living cells using pressure applied via a pipette. *Biophys J* 95:3017–3027.
- Ying LM, et al. (2004) Frequency and voltage dependence of the dielectrophoretic trapping of short lengths of DNA and dCTP in a nanopipette. *Biophys J* 86:1018–1027.

5. Haynes WM, ed (2011) Ionic conductivity and diffusion at infinite dilution. *CRC Handbook of Chemistry and Physics* (CRC Press/Taylor and Francis, Boca Raton, FL), 91st Ed (Internet Version).
6. Lou C, Wang Z, Wang SW (2007) Two-dimensional protein crystals on a solid substrate: Effect of surface ligand concentration. *Langmuir* 23:9752–9759.

7. Smaby JM, Momsen MM, Brockman HL, Brown RE (1997) Phosphatidylcholine acyl unsaturation modulates the decrease in interfacial elasticity induced by cholesterol. *Biophys J* 73:1492–1505.
8. Darst SA et al. (1991) 2-Dimensional crystals of streptavidin on biotinylated lipid layers and their interactions with biotinylated macromolecules. *Biophys J* 59:387–396.

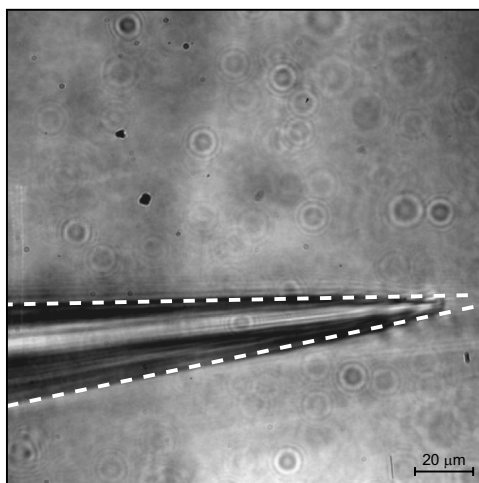


Fig. S1. Image of a conical pipette tip obtained with optical microscopy. The dashed lines delineate the outer surface of the pipette.

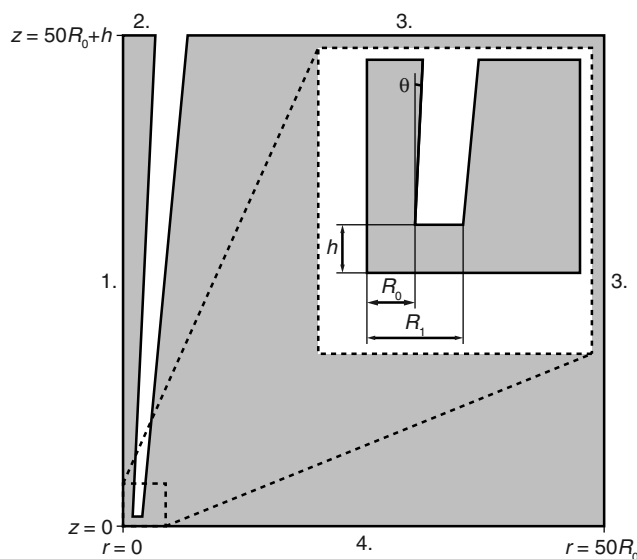
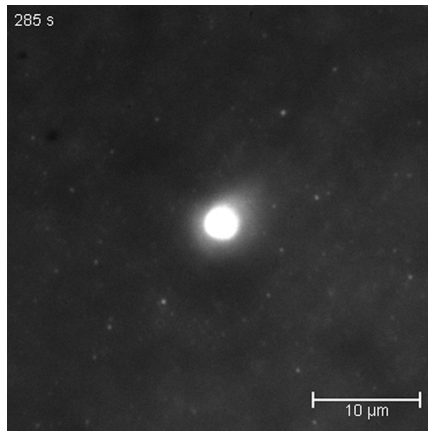
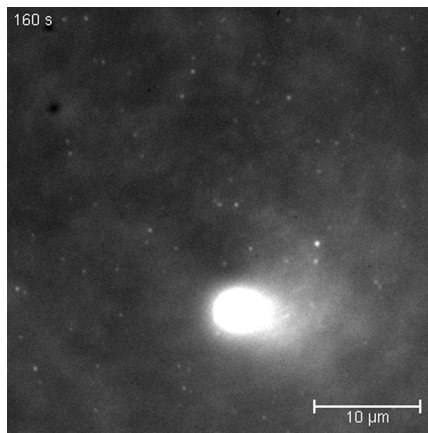


Fig. S2. The geometry used for the finite element simulations, which were solved in cylindrical coordinates  $(r, z)$ .



**Movie S1.** Local accumulation of the fluorescently labeled protein streptavidin by hydrodynamic forces. When the hydrodynamic trap is turned on the protein molecules, which are bound to a supported lipid bilayer, move towards the center of the trap resulting in a local concentration increase. When the trap is turned off the molecules diffuse away and distribute themselves evenly over the lipid bilayer. The trap is turned on and off three subsequent times in the video.

[Movie S1 \(MOV\)](#)



**Movie S2.** Moving trapped molecules in a lipid bilayer. Fluorescently labeled streptavidin molecules are first trapped by hydrodynamic forces as in Supporting Movie S1. By moving the position of the trap laterally the trapped molecules will also move, resulting in local transport of protein molecules in the plane of the lipid bilayer.

[Movie S2 \(MOV\)](#)